UHASSELT
KNOWLEDGE IN ACTION

Maastricht University

Faculty of Medicine and Life Sciences
School for Life Sciences
Master of Biomedical Sciences

Master's thesis

Unravelling the role of reactive oxygen species during epithelial to mesenchymal transition and its link to ferroptosis

Amber Theunissen

Thesis presented in fulfillment of the requirements for the degree of Master of Biomedical Sciences, specialization Molecular Mechanisms in Health and Disease

SUPERVISOR :
Prof. dr. Helena SLAETS

SUPERVISOR :
Dr. Antonio GARCIA DE HERREROS

MENTOR :
Javier PASTOR

2023
2024

Transnational University Limburg is a unique collaboration of two universities in two countries: the University of Hasselt and Maastricht University.

UHASSELT
KNOWLEDGE IN ACTION

www.uhasselt.be
Universiteit Hasselt
Campus Hasselt:
Martelarenlaan 42 | 3500 Hasselt
Campus Diepenbeek:
Agoralaan Gebouw D | 3590 Diepenbeek

UHASSELT
KNOWLEDGE IN ACTION

Maastricht University

Faculty of Medicine and Life Sciences
School for Life Sciences
Master of Biomedical Sciences

Master's thesis

Unravelling the role of reactive oxygen species during epithelial to mesenchymal transition and its link to ferroptosis

Amber Theunissen

Thesis presented in fulfillment of the requirements for the degree of Master of Biomedical Sciences, specialization Molecular Mechanisms in Health and Disease

SUPERVISOR :
Prof. dr. Helena SLAETS

SUPERVISOR :
Dr. Antonio GARCIA DE HERREROS

MENTOR :
Javier PASTOR

Unravelling the role of reactive oxygen species during epithelial to mesenchymal transition and its link to ferroptosis

Amber Theunissen[1,2], Javier Pastor Bautista[2], and Antonio Garcia de Herreros[2]

[1]Faculty of Life Sciences, University of Hasselt, Campus Diepenbeek, Agoralaan building D – B-3590 Diepenbeek
[2] Hospital del Mar Research Institute Barcelona Biomedical Research Park,
C/ Dr. Aiguader, 88 - 08003 Barcelona
ambertheunssen@student.uhasselt.be (A.T.), javier.pastor@upf.edu (J.P.)
Correspondence: Antonio Garcia de Herreros (A.G.H.), Email: agarcia@researchmar.net, Tel: +34 933160433

Running title: role of ROS during EMT

Keywords: Epithelial to mesenchymal transition, reactive oxygen species, N-acetylcysteine, ferroptosis, lipid peroxidation

ABSTRACT

Carcinomas represent the most common type of tumors stemming from epithelial cells which form the lining of organs and tissues throughout the body. These cells have a polygonal shape and are sessile. They form adherent and tight junctions with neighboring cells, depending on the expression of E-cadherin. These epithelial cells can transform into a mesenchymal phenotype, which is characterized by a spindle-like shape, high motility, and replacement of E-cadherin expression by N-cadherin, a conversion known as epithelial-to-mesenchymal cell transition (EMT). This change in phenotype results in migratory and invasive properties and an increased resistance to therapies. Multiple factors can promote this process, including the transforming growth factor-β (TGF-β). The main objective of this study was to determine the lipid peroxidation levels and the role of reactive oxygen species (ROS) in TGF-β-induced EMT using NMuMGs, an epithelial cell line widely used to study this process. Upon EMT, mesenchymal cells showed an increased sensitivity to ferroptosis-induced cell death and a higher production of ROS, which was reduced when cells were treated with N-acetylcysteine (NAC). RNA and protein analysis revealed that NAC did not significantly suppress the expression of mesenchymal markers. However, the migration and invasion assays showed that NAC inhibited the migratory and invasive properties of cells. Further research is still necessary to discover the underlying pathway of ROS interaction in the EMT process, which could contribute to the development of a more specific therapy.

INTRODUCTION

Nowadays cancer is a leading cause of death worldwide, with 18 million new cases and 10 million deaths annually (1). Cell physiological alterations occur and characterize cancer cells promoting self-sufficient growth, insensitivity to anti-proliferative signals, evasion of apoptosis, immune response, tissue invasion, and metastasis among others (2). Metastasis, a hallmark of cancer, is the process in which the primary tumor spreads to other parts of the body and secondary tumors develop, therefore enhancing the malignancy of the cancer. Despite ongoing advancements in the diagnosis and prognosis of these cancers, metastasis remains the predominant cause of mortality, accounting for 90% of all cancer-related deaths. Therefore, a better understanding and further research is necessary to gain more insight into this process (3, 4).

Breast and lung carcinomas are the most prevalent types of epithelial cancers (5). Carcinomas are mainly composed of epithelial cells. These cells form the linings of diverse surfaces throughout the body. These cells serve as a protective barrier against physical, chemical, and microbial damage. Moreover,

epithelial cells typically display a polygonal or cuboidal shape depending on their location and function within the body. These cells are immotile, exhibit an apical-basal polarity, and form strong adherent and tight junctions with neighboring epithelial cells, depending on the expression of E-cadherin (6-8). On the other hand, a tumor also consists of mesenchymal cells. These cells are a type of stromal cells found in connective tissue that can differentiate into various cell types. The morphology of this type of cell is more elongated and spindle-like. Contrary to epithelial cells, mesenchymal cells are motile and invasive, they do not express cytokeratins, but express the intermediate protein Vimentin, and exhibit a front-back polarity. E-cadherin, which is highly expressed by epithelial cells, is replaced by N-cadherin, causing the destabilization of the adherent junctions and tight junctions. Moreover, they attach to the extracellular matrix (ECM) via focal adhesions, making the cells more capable of migrating. Beyond N-cadherin and Vimentin, Fibronectin and Snail1 serve as well as mesenchymal markers (9).

The epithelial cells in the tumor can switch from an epithelial phenotype to a mesenchymal phenotype (10). Whenever this balance is disrupted and there are more mesenchymal cells than epithelial cells, they acquire the capability to invade, resist apoptosis, gain stemness and cellular plasticity, evade immunosuppression, resist chemotherapy, and migrate to distant parts of the body. This phenotypical change is called epithelial-to-mesenchymal transition (EMT) (10).

Accordingly, during EMT, epithelial genes are repressed, and transcription of mesenchymal genes is induced. Foremost, these changes can be induced by the transforming growth factor-β (TGF-β). It is known that cancer cells increase the production of TGF-β (11). It has been shown that augmented expression and activation of TGF-β1 in carcinomas promote an epithelial plasticity response, converting squamous cells in more invasive spindle cell carcinomas. TGF-β exerts its effects by interacting with type I and two type II transmembrane serine-threonine kinase receptors (12). The activation of this pathway results in activation of transcription factors that inhibit or stimulate the transcription of target genes. Subsequently, three families of transcription factors are activated: the Snail1, Twist (member of basic helix-loop-helix family), and zinc-finger E-box-binding (ZEB) families. They are involved in the signaling pathways that initiate EMT in response to TGF-β. First of all, the Snail family exists out of three proteins (Snail1, Snail2, and Snail3) that act as transcriptional repressors. Studies have revealed that in all EMT processes Snail1 induction is observed (13). The primary function of both Snail1 and Snail2 is to suppress the expression of CDH1, which is an epithelial marker gene encoding for E-cadherin. According to *Battle et al.,* silencing of the Snail1 gene restores E-cadherin levels (14). However, Snail1 and Snail2 do not only suppress E-cadherin, but also inhibit the expression of genes that play a role in maintaining the epithelial structure and function, such as the genes encoding Claudins and Occludins. Similar to Snail, the ZEB family also represses E-cadherin directly and they initiate a delocalization of β-catenin (13). Lastly, according to *Yang et al.,* ectopic expression of Twist decreases E-cadherin, Occludin and, Claudin expression while increasing the expression of Vimentin and N-cadherin (11, 15). In summary, TGF-β induces the production of transcription factors (e.g., SNAIL, TWIST, ZEB) and these factors will regulate the transcription of genes involved in EMT by repressing or stimulating their expression.

Upon activation of these transcription factors EMT occurs. EMT is involved in various aspects of tumorigenesis (16). To begin with, EMT is associated with the acquisition of stem cell- like properties. Pluripotency-related genes are activated by the expression of Snail1 (e.g., HDAC1, Oct4, etc.) in several cancers (17, 18). Resistance to apoptosis is another consequence of EMT caused by the repression of the pro-apoptotic gene PTEN and others (19). Moreover, it has been previously described in our lab that overexpression of Snail1 modulated cisplatin resistance of colon cancer cells. HT29-M6 overexpressing Snail1 are less sensitive to cisplatin treatment suggesting that Snail1 expression causes chemoresistance contributing to tumorigenesis (20). As previously mentioned, Snail1 inhibits the expression of E-cadherin, destabilizing the junction between neighboring cells and providing the cell with the opportunity to migrate and spread to other parts (21). The next steps in tumorigenesis when the cells are able to migrate, are to invade the bloodstream and spread to other parts of the

body. It has been described by *Chang et al.,* that the expression of VEGFA and endothelial markers, such as CD105, CD31, and VEGFR1 is upregulated when Snail1 expression is increased. These markers play an important role in initiating angiogenesis (22). In brief, upregulated levels of Snail1 caused by the initiation of EMT, promote tumorigenesis by creating chemoresistance, activating apoptosis resistance mechanism, migration, invasion, and metastasis.

Ferroptosis is a type of cell death that relies on intracellular iron-dependent lipid peroxidation and accumulation of reactive oxygen species (ROS), which is different from apoptosis, necrosis, and autophagy. Only newly, this nonapoptotic pathway was referred to as ferroptosis (23). Others described that erastin, an oncogenic RAS-selective lethal small molecule, triggers a distinct lethal pathway, which differs from commonly regulated cell death pathways (23, 24). It is known that mesenchymal cells are more resistant to various types of cancer treatments. However, studies have revealed that these resistant cancer cells in a mesenchymal state are more sensitive to ferroptosis induced cell death (25). Ferroptosis is dependent on lipid peroxidation, which relies on three factors: ROS, iron metabolism, and oxidative lipids.

Primary, increased levels of oxidizable lipids, more specifically polyunsaturated fatty acids (PUFAs), lead to lipid peroxidation in the presence of ROS. When lipid peroxidation occurs, a bisallylic hydrogen atom will be removed from in between two carbon-carbon double bonds from poly unsaturated fatty acyl moieties present on phospholipids (PUFA-PL) embedded in the lipid bilayers. This structure forms a carbon-centered radical and reacts with molecular oxygen causing the formation of lipid radicals, namely phospholipid hydroperoxides (PLOOHs). An increase in PUFA levels increases the sensitivity to ferroptosis (26). Furthermore, ferroptosis is dependent on iron. A key player in this process is the non-enzymatic iron-dependent Fenton chain reaction. This reaction causes a reaction between PLOOHs and ferrous ions, leading to the production of free radicals such as PLO* and PLOO* (27, 28). Therefore, these free radicals accumulate, contribute to membrane damage, eventually leading to cell death. Typically, cancer cells have the ability to evade cell death mechanisms and resist ferroptosis by expressing glutathione peroxidase 4 (GPX4), a selenoprotein that protects against overabundant lipid peroxidation (29). Another gene that is involved in protecting against ferroptosis is ferroptosis suppressor protein I (FSP1) (30). More specifically, GPX4 reduces PLOOHs to alcohols in the membranes (29). By inhibiting GPX4 by using either RSL3, an indirect inhibitor, or erastin, an indirect inhibitor, the PLOOHs will not be neutralized (31). According to *Vasanthi et al.,* the mesenchymal cells are more vulnerable to ferroptosis. They suggested that the mesenchymal transcription factor ZEB1 plays a role in the lipid metabolism by regulating PPARγ, a key regulator of lipid metabolism, to produce higher levels of PUFAs. Additionally, knockout of ACSL4 and LPCAT3, upstream regulators of PUFA metabolism and inhibition of lipoxygenases decreased the functionality of GPX4 and hindered cell death (25).

Finally, the last key player in ferroptosis are ROS. In this process of cell death, high levels of ROS are observed owing to an imbalance in the redox state (32). Lipid peroxidation occurs via the Fenton reaction, which requires ROS to form PLOOHs.

The roles of ROS and lipid peroxidation during EMT are understudied. A study conducted by *Lui et al.,* investigated the relationship between ROS and TGF-β. They discovered that ROS activates the TGF-β pathway by stimulating various pathways, including the Smad pathway (33). As mentioned previously, TGF-β is an inducer of the mesenchymal phenotype. This study might suggest that ROS might be involved in EMT, making the mesenchymal cells more vulnerable to ferroptosis (33).

Therefore, the goal of this project is to investigate what will happen with the lipid peroxidation during EMT and to discover the role of ROS during EMT. The different aspects of tumorigenesis will be investigated upon treatment with antioxidants such as N-acetylcysteine (NAC) or tocopherol.

Once this is achieved, these findings could be used to understand to interaction between ferroptosis and EMT, which could lead to overcoming the resistance of mesenchymal state cancer cells to therapies.

EXPERIMENTAL PROCEDURES

Cell lines.

NMuMGs, from the cell bank of PRBB were grown under either high glucose (4.5 g/l) Dulbecco's modified Eagle's medium (DMEM) (Invitrogen) or low glucose (1 g/l) DMEM supplemented with 10% fetal bovine serum (FBS), 100 units/ml penicillin, 100 ug/ml streptomycin, 2 mM glutamine and 10 ug/ml insulin. All cells were maintained in a humidified incubator at 37°C in the presence of 5% CO_2 and 95% atmospheric air. To stimulate the NMuMGs to induce EMT, cells were treated with TGF-β (5 ng/ml).

HT29-M6, intestinal tumor cells were provided by the cell bank of PRBB. To obtain an overexpression of Snail1 these cells were transfected (34). Cells were cultured in DMEM (Invitrogen) supplemented with 10% FBS in an atmosphere of 5% CO_2.

MTT viability assay.

2 x10^4 cells/well were seeded in a 96 plate, incubated for 24 h with DMEM 10% FBS. Depending on the experiment, cells were treated with TGF-β and the FBS was reduced to 1%. Subsequently, after 24 h the cells were treated with the treatment of interest. After incubation time, 100 μl of 3-(4,5-Dimethylthiazol-2-yl)-2,5-Diphenyltetrazolium Bromide (MTT) solution (5 mg/ml in PBS) (MTT, Sigma-Aldrich) in 0% FBS were added to each well and then kept for 3 h at 37°C in darkness. Next, the solution was removed and 100 μl of Isopropanol: DMSO (4:1) were added to each well. After 15 min, the absorbance was measured at 590 nm in an infinite M200 microplate reader (TECAN).

RNA extraction and Real-time RT-PCR.

Cultures were washed twice with cold PBS (4°C), Trizol reagent (Invitrogen) was added to lysate the cells using scrappers. After lysate collection, 200 μl of chloroform was added, and samples were centrifuged at 12000 rpm for 20 min at 4°C. Next, the aqueous phase at the top, was collected and 500 μl of isopropanol was added to each sample. Samples were incubated at room temperature for 15 min, and then centrifuged again at 120000 rpm for 20 min at 4°C. A solid pellet should precipitate at the bottom, subsequently the supernatant is removed and 1ml of ethanol is added. Before centrifuging, samples were vortexed to clean the pellet. Following that, the supernatant was removed, and the pellet was resuspended in 20ul of H_2O. Lastly, the samples were quantified using Nanodrop 1000 (Thermo scientific) and either stored at -80°C or reverse transcribed.

Next, RNA was reverse transcribed using transcription First strand cDNA synthesis kit (Roche). Then, 40 ng of cDNA was amplified in triplicates using Light cycler 480 Real Time System (Roche). Values were normalized to the expression of housekeeping genes (Pumilio). The primers used are listed in supplementary table 1.

Invasion and migration assay

To demonstrate the migration and invasion properties, cells were seeded in a 90 x 20 mm plate (DMEM 10% FBS). After 24 h the FBS was reduced to 1%, NMuMGs were activated with TGF-β and if necessary, treated with the drug of interest for 24 h. Subsequently, 50,000 cells were seeded in 0,2% FBS- 1% BSA in each trans well filter chamber (Costar3422) and 10% of FBS was added in the lower chamber. Before seeding the cells for an invasion assay, the Transwells were coated with 45 μl of Matrigel 0,5 μg/ μl (354230, Corning). After 8 h for migration and 18 h for invasion, the Transwells were washed three times with PBS, fixed with methanol (-20°C) and stained with crystal violet (0,5% crystal violet in 25% MetOH in H_2O) for 10 min. Again, three washes with PBS were done and the remaining non migrating cells were cleaned with a cotton swap. Lastly, the membrane of the Transwell is obtained, dissolved in 150 μl of 30% of acetic acid and the absorbance was measured with the infinite M200 microplate reader (Tecan).

ROS analysis

To analyze the levels of ROS, 25,000 cells were seeded in each well of a 96 clear bottom white plate. After 24 h, FBS was reduced to 1% and cells were treated with the drug of interest. A specialized kit (Abcam, ab113851) was used to determine the levels of ROS. According to this protocol, cells were incubated for 1h at 37°C in the dark with DCFDA (2' ,7' - dichlorofluorescin diacetate). The signal is measured with the infinite M200 microplate reader (Tecan) at different times and data was normalized by the number of cells.

Western Blot.

To extract and quantify protein of the samples, cells were washed twice in cold phosphate-buffered saline (PBS) and lysed in 1% lysis buffer (SDS 2%, glycerol 10%, 50 mM tris pH 7,5). Samples were heated for 15 min at 95°C and centrifuged at 12000 rpm for 5 min at 4°C. Protein concentration was determined using DC protein assay reagent kit (Bio-rad) using a standard curve of 0-12 μg bovine serum albumin (BSA). Absorbance was measured using an infinite M200 microplate reader (TECAN) at a wavelength of 590 nm.

Prior to sample preparation, SDS-gels of 10-12% were prepared. Next, samples were prepared by addition of sample buffer 5x. Consequently, samples were boiled at 95°C for 5 min. Proteins were separated for 90 min at a voltage of 100V in electrophoresis buffer 5x (25mM Tris, 192 mM glycine, 0.5% SDS). Subsequently, electro transfer of proteins onto a polyvinylidene difluoride (PVDF) membrane at 100 v in cold transfer buffer 5x (25mM Tris, 192 mM glycine, 10% methanol) for 60 min. Before overnight incubation at 4°C with the primary antibody, the membrane was blocked with TBS-T buffer (25mM Tris-HCl, 137 mM NaCl. 0,1% tween 20) in 1% BSA for 45 min. Following overnight incubation, three washes were done with TBS-T for 5 min and then incubated with the secondary antibodies peroxidase-combined (HRP) for 1 h 30 min at RT. Lastly, to develop the membranes, three washes were done with TBS-T and incubated with immobilon ®Western Chemiluminescent HRP substrate (Millipore). Membranes were analyzed in Alliance Q9 (UVITEC) chemiluminescence imager and quantified using ImageJ software.

Lipid peroxidation determination

The following protocol was used to determine the lipid peroxidation levels. First, cells were washed with PBS, incubated with trypsin for 10 min at 37°C and neutralized with DMEM 10% FBS. Next, the cells were centrifuged at 350 g at 4°C, the supernatant was removed, and cells were resuspended in DMEM 1% FBS. Samples were present in duplicates, one of them was stained with 5 μM of BODIPY^{TM} 581/591 (Thermo Fisher) and the other one was used to remove unspecific signal. The samples were stored on ice and read with Flow Cytometer Analyser using FITC 530/30 filter.

Spheroids assay

400 cells in a volume of 30μl of high glucose DEMEM 10% FBS and insulin (1:100) were seeded in droplets in the lid of a plate for 24 h and DMEM 10% FBS was added in the bottom of the plate. Next, 140 μl of the following mix: 90 μl collagen I (4 mg/ml) + 15 μl NaOH (0.1 M) + 195 μl DEMEM without FBS was added in a 24 well plate for 10 min. Then 4-5 droplets of cells were added in each well and again after 10 min 140 μl of the previous described mix was added. Droplets were analyzed daily with Inverted microscope Axio Vert.A1.

Statistical analysis

All experiments were conducted representative from at least three independent repetitions. Data are presented as mean ±SD. Statistical analysis was performed using GraphPad Prism Software. Data were analyzed for significance using an Unpaired T-test or analysis of variance (ANOVA). P-values < 0,05 are indicated with one asterisk.

RESULTS

NMuMGs under low glucose conditions seem to exhibit more mesenchymal characteristics compared to NMuMGs cultured under high glucose conditions.

NMuMGs are highly sensitive to changes in glucose levels. For this reason, we investigated different characteristics related to EMT and compared high glucose (4.5 g/l) and low glucose conditions (1 g/l). To analyze the mesenchymal protein expression levels, a western blot analysis was performed.

Figure 1A reveals that after three hours of TGF-β treatment, the levels of Snail1 were increased under low glucose conditions compared to those under high glucose conditions. GPX4 showed no differences in expression after three hours of treatment with TGF-β. However, after overnight treatment (ON) the levels were decreased. After ON treatment with TGF-β, the protein levels of fibronectin increased more in low glucose conditions than in high glucose conditions. It is known that EMT contributes to the migration capabilities of the cells. A Transwell migration assay revealed that both, epithelial and mesenchymal cells migrated more in low glucose conditions. Based on these

experiments, we decided to focus on low glucose conditions.

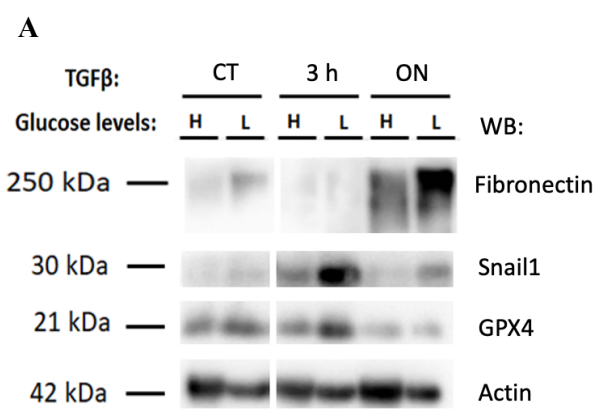

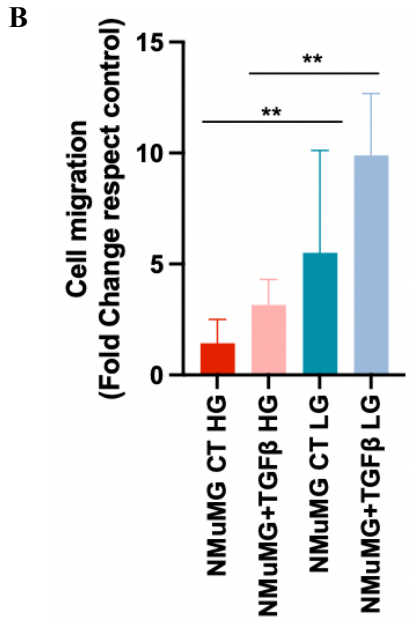

Fig. 1. NMuMGs under low glucose conditions migrate more and show higher protein levels of fibronectin and Snail1. (A)Western blot analysis of mesenchymal markers upon treatment with TGF-β (0 h, 3 h, and ON) under high and low glucose condition. (B) Transwell migration assay under high and low glucose of epithelial and mesenchymal cells. Data are means $\pm$ SEM (n=3). Significant differences were evaluated by Student's T-test. **P<0.01.

Mesenchymal cells were more sensitive to ferroptosis-induced cell death by RSL3 and erastin.

To validate the findings described in previous studies that mesenchymal cells are more sensitive to ferroptosis, MTT viability assays of NMuMGs were performed with RSL3 and erastin. Both epithelial and mesenchymal cells were treated with either one of the ferroptosis inducers, RSL3 or erastin. Figure 2A and B show that the mesenchymal cells have a significantly decreased cell viability compared to epithelial cells upon increasing the concentration of RSL3 and erastin. The cell viability of epithelial cells remained almost 100% when treated with RSL3 0.25 μM while the viability of the mesenchymal cells was reduced to almost 0%. A similar reduction in viability was observed when the cells were treated with erastin 1 μM. Then, the mesenchymal cells were treated with the antioxidant tocopherol, and this recovered the decreased cell viability induced by RSL3 (Fig. 2C). Thus, these data suggest that mesenchymal cells are more sensitive to ferroptosis-induced cell death by RSL3 and erastin.

The lipid peroxidation levels are higher during EMT.

As ferroptosis relies on lipid peroxidation, the peroxidation levels were determined in epithelial and mesenchymal cells upon induction of EMT. No differences were observed in lipid peroxidation levels upon treatment with RSL3 or erastin in NMuMG control cells. To determine whether ROS might play a role in this process, the CT cells were treated with the antioxidant tocopherol. No reduction in lipid peroxidation was detected after tocopherol (Fig 3 A). Hydrogen peroxide (H_2O_2) was used as a positive control because it is able to induce lipid peroxidation (35). However, when the NMuMGs were treated with TGF-β and became mesenchymal the lipid peroxidation levels significantly increased and peroxidation levels resembled those of epithelial CT cells. These findings suggest that there is increased lipid peroxidation in mesenchymal cells which are more sensitive to ferroptosis (Fig. 3B).

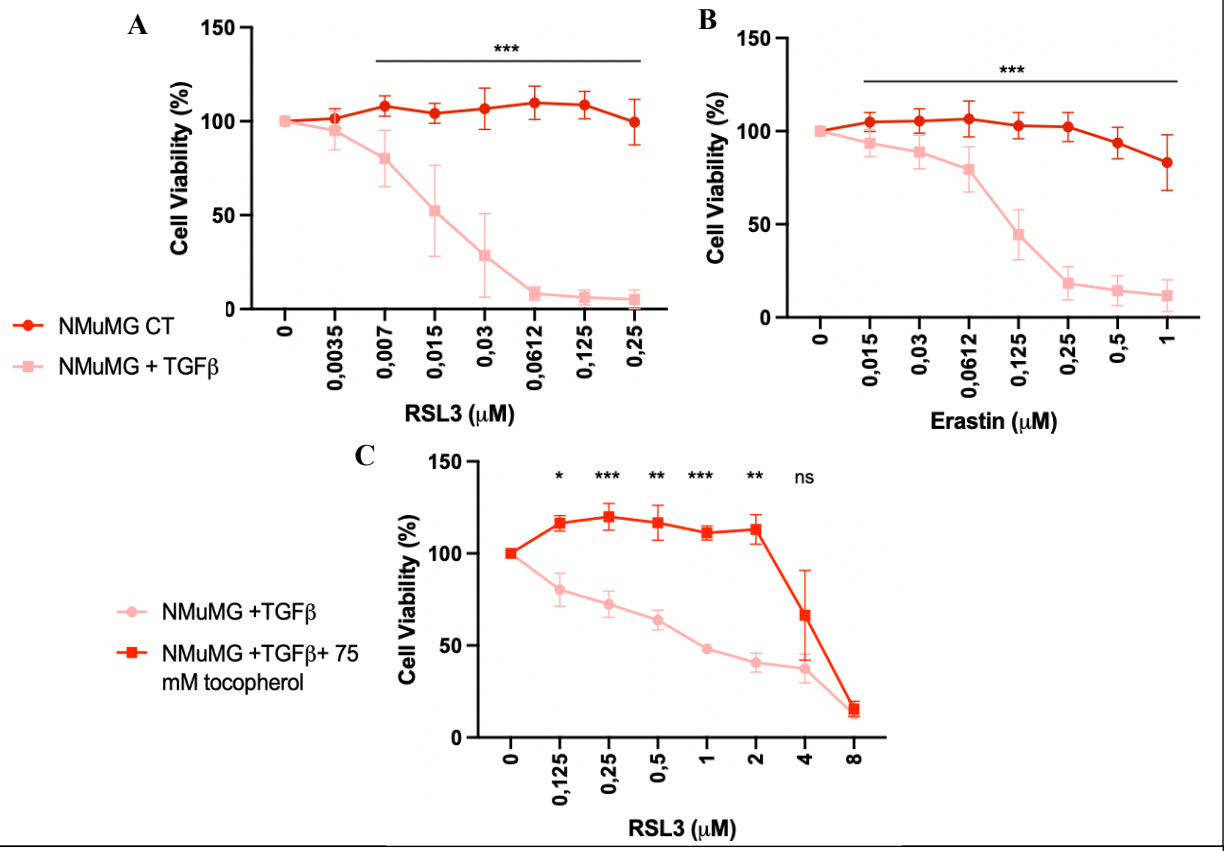

Fig. 2– Mesenchymal cells are more sensitive to ferroptosis-induced cell death by RSL3 and erastin. (A) Viability of NMuMGs CT and NMuMGs + TGF-β treated with RSL3 (0.5 μM)(n=4). (B) Viability of NMuMGs CT and NMuMGs + TGF-β treated with erastin (2 μM) (n=5) (C) Viability of NMuMGs + TGF-β $\pm$ tocopherol (75 μM) treated with RSL3 (0.5 μM) (n=3) Data are means $\pm$ SEM. Significant differences were evaluated by Student's t test. * P< 0.05, **P< 0.01 and ***P< 0.001.

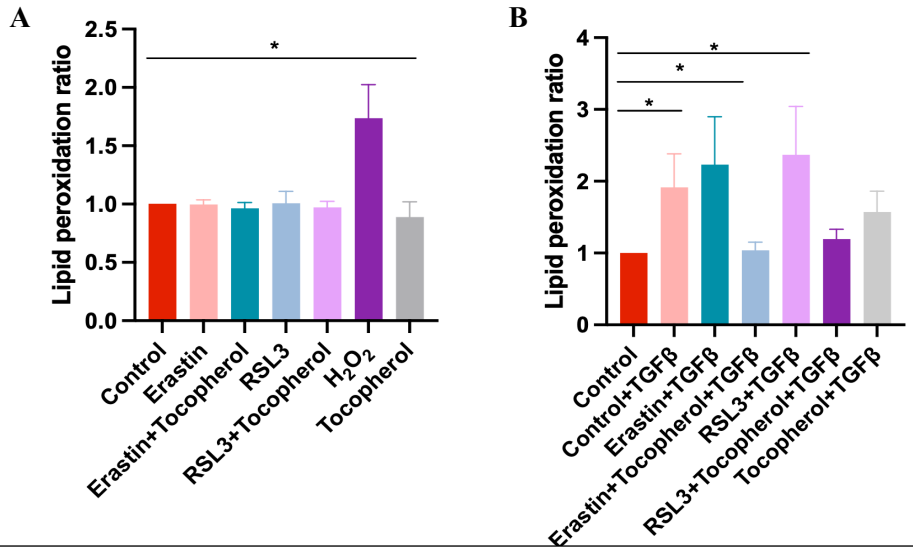

Fig. 3– Mesenchymal cells have higher lipid peroxidation levels compared to epithelial cells. (A) Lipid peroxidation levels of NMuMGs treated with either RSL3 (0.5μM) or erastin (2 μM) $\pm$ tocopherol (75 μM), H_2O_2 (25 μM) as a positive control and the antioxidant as a negative control. (B) Lipid peroxidation levels of mesenchymal cells treated with either RSL3 or erastin $\pm$ tocopherol. Data are means $\pm$ SEM (n=3). Significant differences were evaluated by Student's t test. *P<0.05. H_2O_2; Hydrogen peroxide.

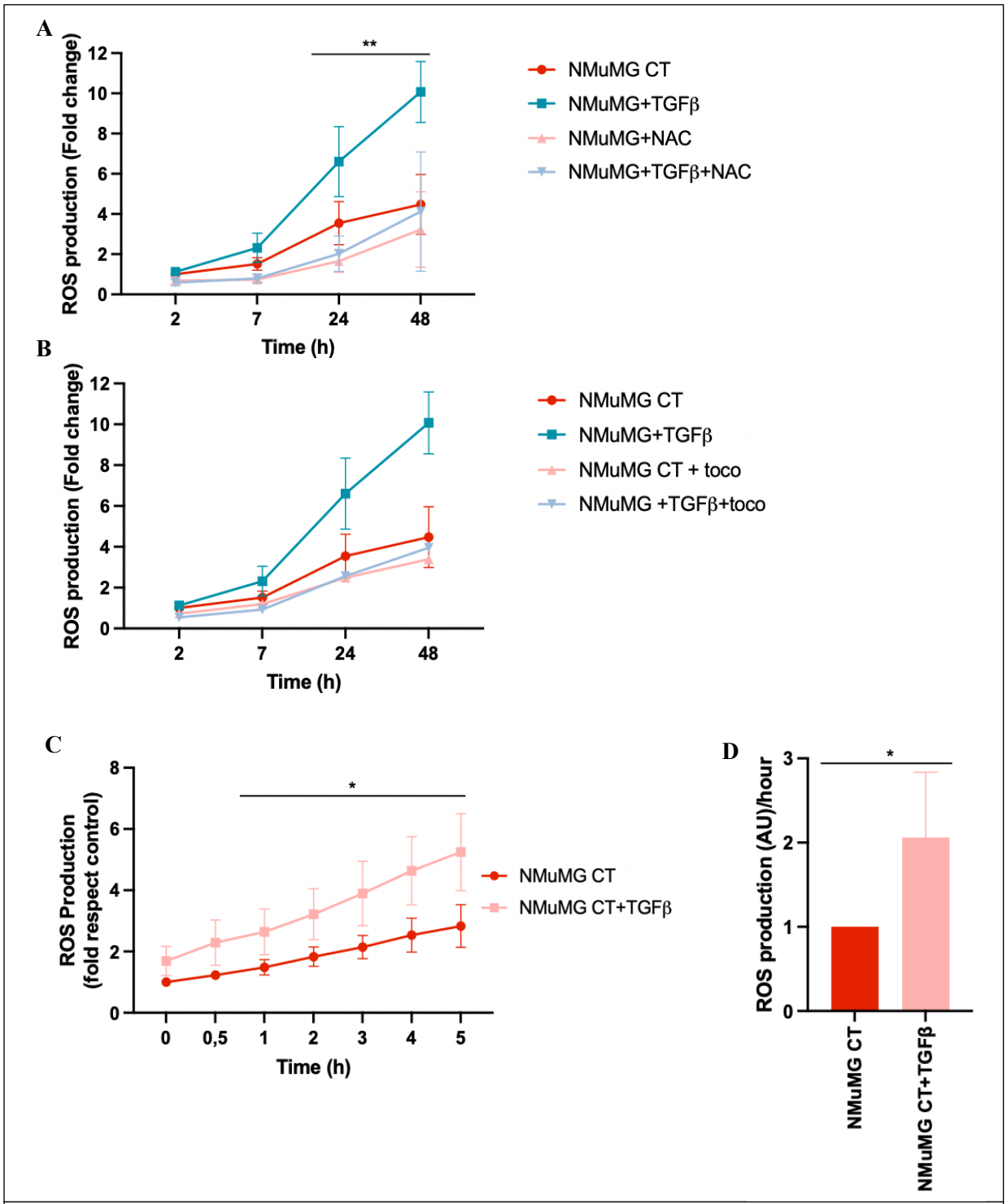

Fig. 4– Mesenchymal cells exhibit higher ROS levels compared to epithelial cells in LG. (A) ROS levels during EMT starting from 2 h until 48 h after EMT ± NAC (0.75 *mM*) (n=3). (B) ROS levels during EMT starting from 2 h until 48 h after EMT ± tocopherol (n=1). (C) ROS production levels 24 h after EMT was induced (n=4). (D) ROS production levels per hour (n=4). Data are means ± SEM. Significant differences were evaluated by analysis of variances (ANOVA). *P<0.05, **P<0.01, n=4 ROS; reactive oxygen species, CT; control, NAC; N-acetylcysteine

Mesenchymal cells produce higher levels of ROS during EMT compared to epithelial cells and this increase is reverted upon treatment with NAC.

The levels of ROS were determined in epithelial and mesenchymal cells using the Abcam ROS kit to evaluate the differences in ROS upon EMT. As shown in Figure 4A & B

the ROS levels were measured starting from the induction of EMT. As shown in Figure 4A, the ROS levels at 2 - 7 h after EMT induction were only slightly increased, but no significant difference was observed between NMuMG CT cells and NMuMG + TGF-β. However, seven hours after EMT induction the production of ROS was greater, and after 24 h, this increase was even greater. Compared to mesenchymal cells, epithelial cells produce lower levels of ROS. This increase was prevented when the antioxidants, NAC and tocopherol, were added (Fig. 4A and B). Figure 4C shows the ROS levels measured starting 24 h after EMT induction. After 24 h, ROS production levels continued to increase and there was a significant difference in production between epithelial and mesenchymal cells. Finally, the ROS production was calculated per hour (Fig. 4D) and mesenchymal cells produced significantly more ROS per hour than epithelial cells. The experiments described here were performed in low glucose. Supplementary Figure 1 shows the same results for ROS production under high glucose conditions.

NAC inhibited the invasion and the capability of digesting the membrane matrix.

To assess the role of ROS in EMT, we performed invasion assays using Transwells. As shown in Figure 5, mesenchymal cells invaded twice as much as epithelial cells. When the epithelial cells were treated with NAC, their invasion capabilities were slightly inhibited. In contrast, when the mesenchymal cells were treated with NAC, their invasion capabilities were reduced to approximately 50%. To test the influence of NAC on the migration capabilities, a Transwell migration assay was performed on the epithelial cells and upon treatment of NAC, it was observed that these epithelial cells migrated less (Fig. 2BS)

Next, to assess whether NAC could prevent the digestion of the membrane matrix, a spheroid assay was performed. In this assay, we determined the digestion capability of cholesterol in the membranes. Microscopic imaging (Fig. 5B) revealed that NMuMG cells grew in a nicely lined group. When the cells were treated with TGF-β for 48 h, more individual cells were identified, the membrane of the spheroid was disrupted, and various cells expanded to the environment. However, this disruption was reversed when mesenchymal cells were treated with NAC, and they resembled epithelial cells. Moreover, after 120 h of TGF-β treatment, the cells spread even further when the membrane was disrupted. Upon treatment with NAC, the cells were again nicely lined, and all the cells grew in the spheroid. This difference was even greater.

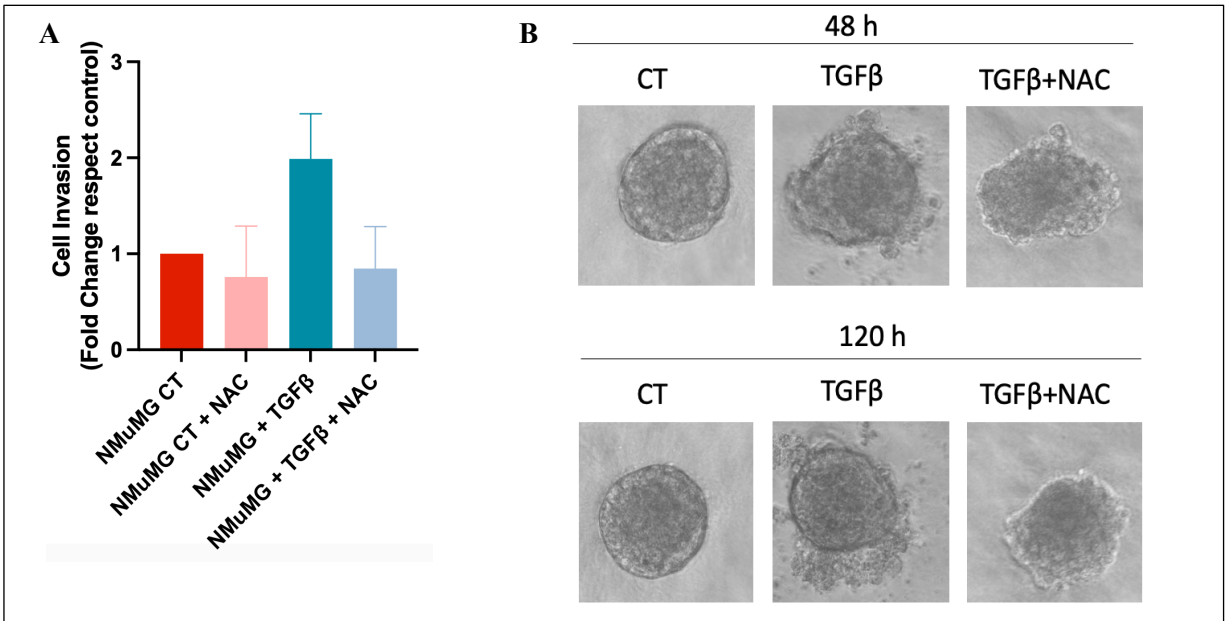

Fig. 5– NAC inhibits invasion capabilities of and reduces the ability to digest the membrane of NMuMGs. (A) Transwell invasion assay of NMuMG control cells and cells treated with TGF-β $\pm$ NAC (0.75 *mM*). after 24 h (n=2). (B) Spheroid assay of NMuMG control cells and NMuMG + TGF-β cells treated with NAC for 48 h and 120 h with Axio Vert.A1 microscope. (objective 50 x).

The expression of some mesenchymal markers was only slightly modified by NAC at the RNA level, and no differences were observed at the protein level.

To better understand why mesenchymal cells produce higher levels of ROS, gene and protein expression levels were investigated during EMT. The microscopic images show that the phenotype of epithelial and mesenchymal cells varies. Mesenchymal cells have a more spindle-like shape, whereas the epithelial cells exhibit a polygonal shape. However, when mesenchymal cells were compared to mesenchymal cells that were treated with NAC, there was no clear difference seen in the phenotype (Fig. 6A).

The next step was to determine whether there were differences at gene expression levels. qPCR analysis revealed in Figure 6B that upon treatment with NAC mesenchymal markers, such as *Vim* and *Cdh2,* were only slightly inhibited. There was no effect of NAC on *Cdh1*, an epithelial marker. Protein levels were analyzed using western blotting (Fig. 6C). The NMuMGs were treated with or without TGF-*β* and NAC. The protein levels of Fibronectin and Vimentin were higher in mesenchymal; however, there was no difference when the cells were treated with NAC. Epithelial marker, E-cadherin was upregulated in epithelial cells, and no difference was seen upon treatment with NAC. Supplementary Figure 2A shows a qPCR in high glucose, which reinforces the findings that NAC does not affect the gene expression and protein levels upon EMT.

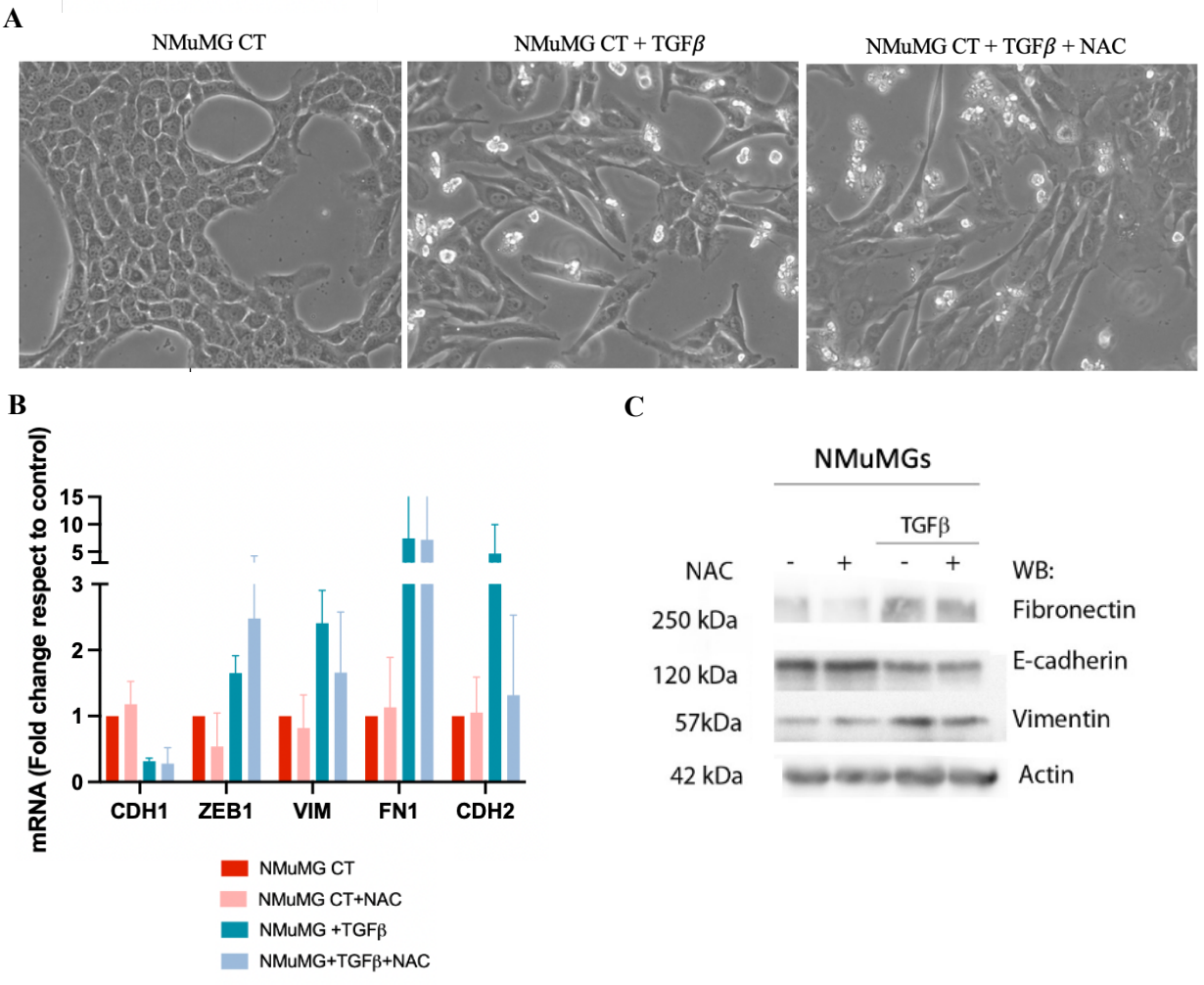

Fig.6 –NAC does not affect mRNA and protein levels of epithelial and mesenchymal markers. (A) Microscopic image of NMuMGs CT, +TGF-*β*, TGF-*β* + NAC with Axio Vert.A1 microscope. (objective 20 x). (B) qPCR plot of NMuMGs revealing the expression of mesenchymal markers (*Zeb1*, *Vim*, *Fn1* and *Cdh2*) and epithelial marker (*Cdh1*) in low glucose (n=3). (C) Protein expression of fn1, cdh1, vim, and actb showed by western blot.

DISCUSSION

Epithelial-to-mesenchymal transition (EMT) is a process that occurs in cancer cells. Epithelial cells change their phenotype to become mesenchymal cells (6). Studies have shown that the mesenchymal phenotype contributes to metastasis by activating the migration, invasion, and other processes involved in tumorigenesis. Moreover, it is observed that these mesenchymal cells are more resistant against current chemotherapies (16, 20). Furthermore, research indicates that the mesenchymal cells are more sensitive to a type of programmed cell death referred to as ferroptosis (36). The process of ferroptosis relies on three factors; ROS, lipid peroxidation, and iron (26). The reason why these mesenchymal cells are more sensitive to ferroptosis is, yet unknown, and further research is necessary to gain more insights into interaction between the process of ferroptosis and EMT. Once this is achieved, it could help overcome the resistance of mesenchymal-state cancer cells to therapies and the development of more targeted therapies. In this study, we investigated the two factors involved in ferroptosis; lipid peroxidation and ROS during EMT.

First, it was important to determine the optimal conditions for performing our experiments. Western blot analysis and migration assays revealed that the NMuMG cells were more mesenchymal under low glucose conditions, with higher protein levels of Snail1 after the first three hours after EMT induction. These levels decrease overnight because Snail1 plays a primary role during the EMT (37). Fibronectin levels increased after 24 h, and there was a higher migration rate of cells under low glucose conditions. The human body has a blood glucose concentration between 0.7 g/l and 1 g/l which is physiologically more comparable to the composition of low glucose media (1 g/l) (38). Additionally, glucose is a substrate for the phosphate pentose pathway (PPP), which produces nicotinamide adenine dinucleotide phosphate (NADPH) that is involved in the redox homeostasis (39, 40). NADPH is required for the assembly of reduced glutathione (GSH) responsible for the reduction of ROS (41). When cells grow under high glucose conditions, this pathway is stimulated, and ROS levels are reduced. If our hypothesis is correct and ROS play a role during EMT, this process will be inhibited through the scavenging of ROS, suggesting that the low glucose is the best condition for this study.

The results of the viability assays to determine the sensitivity to ferroptosis inducers showed that mesenchymal cells were more sensitive to ferroptosis-induced cell death by RSL3 and erastin. This validates the findings of *Viswanathen et al.* (25). These results may be due to the fact that mesenchymal cells have increased levels of transcriptional factors such as Snail1, Twist and Zeb1 (42, 43). Studies have revealed that Zeb1 inhibits GPX4 transcription by binding to the E-box motif, leading to the accumulation of ROS, which is one of the necessities for ferroptosis. Furthermore, PPARγ expression is in induced by Zeb1, which affects the lipid metabolism. It regulates the uptake and accumulation of lipids, more specifically PUFAs, and it plays a role in the membrane remodeling that occurs during EMT at the PUFA oxidation site (43). In conclusion, all of these factors play a role in sensitizing the mesenchymal cells to ferroptosis.

Next, to assess whether the cells died through ferroptosis, we studied the lipid peroxidation levels, which is a specific marker of ferroptosis. This experiment showed that the epithelial cells did not show any changes in lipid peroxidation levels upon treatment with RSL3 or erastin (ferroptosis inducers). These results validated the results of the viability assay, which showed that epithelial cells were not sensitive to ferroptosis-induced cell death. However, when the mesenchymal cells were treated with RSL3 or erastin, there was an increase in lipid peroxidation, suggesting that the cells die trough ferroptosis. To confirm that the cells are undergoing ferroptosis rather than another form of cell death, future studies should be conducted using ferroptosis inhibitors. Ferroptosis inhibitors used in studies are liproxstatin-1 and ferrostatin-1 (44, 45). These findings suggest that EMT induces alterations that affect lipid peroxidation. Our hypothesis posits that ROS might play a role in this process.

To further investigate our hypothesis, ROS levels were quantified after the induction of EMT. It is seen that mesenchymal cells produce higher levels of ROS than epithelial cells. The first seven hours after TGF-β treatment, there was no increase in ROS production. A significant increase was observed after 24 h. According to different protocols, after 24 h of treatment with TGF-β, the

NMuMGs performed the EMT, exhibiting a mesenchymal phenotype (46, 47). This suggests that ROS are a consequence of EMT rather than a requirement to perform EMT. That the ROS production levels are increased in mesenchymal cells may be due to TGF-β. TGF-β causes an increase in ROS by hindering mitochondrial function promoting NADPH oxidases (NOX). According to *Boudreau et al*., knockdown of NOX4 inhibited TGF-β induced cell migration (48). Additionally, it will repress antioxidant systems, such as GSH leading to oxidative stress and a redox imbalance (33, 49). When the cells were treated with the antioxidant NAC, the levels of ROS in mesenchymal cells were reduced and resembled the epithelial levels. NAC is a precursor of reduced GSH that neutralizes free radicals such as OH and H_2O_2 by donating a sulfhydryl group (50). The use of NAC to decrease the ROS production may inhibit EMT.

Then, the effect of NAC on different aspects of tumorigenesis was investigated, such as invasion and the ability of the cells to degrade the membrane matrix. The Transwell invasion assay revealed that NAC inhibited the invasion capabilities of mesenchymal cells by approximately 50%. Additionally, the spheroids assay showed that mesenchymal cells disrupted the matrix and were able to spread outside the spheroid. However, when the mesenchymal cells were treated with NAC, the matrix remained intact. During EMT, the migratory and invasive properties of epithelial cells are activated upon loss of adhesion to their neighbors (51). *Chen et al.,* described a mechanism in which ROS is involved in the activation of migration and invasion upon cell-cell adhesion loss (52). The Rho (ρ) protein family plays a role in cell-cell adhesion junctions and migration (53). Normally, inhibition of Rac1 stabilizes adherent and tight junctions because of the binding of TIAM1 to these junctions. Upon loss of the junctions, TIAM1 is released, and Rac1 is activated. This promotes ROS generation, leading to the activation of pathways promoting migratory and invasive factors (54). NAC reduces the levels of ROS and inhibits this machinery.

Lastly, it was interesting to investigate whether NAC had an effect on epithelial and mesenchymal markers at the mRNA and protein levels because of the ability of NAC to modify the invasion capacities observed in the previous results. First, the histological images did not show any phenotypic changes when mesenchymal cells were treated with NAC, and they were similar to the mesenchymal cells that were only treated with TGF-β. mRNA analysis using qPCR revealed that some mesenchymal markers, Vimentin and N-cadherin may be slightly decreased upon treatment with NAC, but this was not significant. Protein analysis showed that there were no differences in the protein levels when the cells were treated with NAC. The cells were treated for 24 h with NAC (0.75 mM), and the concentration of NAC might have been too low to observe an effect on mRNA and protein levels. *Song et al.,* investigated the effect of NAC on TGF-β-induced EMT in human renal tubular cells (HK-2) and used a concentration of 5mM (55). A future step could be to determine the viable concentration of NAC and investigate whether this could influence the mRNA and protein levels. Another aspect that can be modified is the treatment time. It is possible that, 24 h of treatment with NAC is not sufficient in NMuMGs to observe its effect. Additional pretreatments may be a solution. Several studies have treated the cells with NAC for 1 h before treatment with the drug of interest with an incubation time of 48 h or 72 h (56, 57). It might also be interesting to identify other genes and proteins involved in different aspects of tumorigenesis that could be modified by ROS instead of focusing on genes involved in the induction of EMT because NAC was not able to revert the mesenchymal phenotype. These genes could include genes encoding Matrix Metalloproteinases (MMPs), which cause the breakdown of the extracellular matrix (ECM) (58). Other genes include Zeb1, which inhibits GPX4, CXCR4, a chemokine receptor, and integrins, which are involved in cell-ECM adhesion (59). As previously discussed, the Rho gene family is implicated in cellular migration and the regulation of cell-cell adhesion junctions. Therefore, investigating the expression levels of the Rho genes upon treatment with NAC may be interesting (60).

Future research could include the identification of all the proteins and genes that may be modified by ROS and their roles in the EMT. These genes and proteins could be involved in invasion of cells and the cell-cell adhesion. It would be interesting to investigate these findings in a cancer cell line to increase their translational value. Eventually when there is a better understanding of in which part ROS plays a role

during EMT, underlying downstream mechanisms and pathways should be investigated.

CONCLUSION

From this study we can conclude that the mesenchymal NMuMGs are more sensitive to ferroptosis-induced death based on the increased lipid peroxidation levels in these cells and the increased levels of ROS production. Moreover, ROS influences the invasion capabilities of NMuMGs. Decreasing the levels of ROS by treating the cells with NAC inhibited the invasion and the capability to digest the membrane. However, upon treatment with NAC there is no phenotypical change observed suggesting that NAC cannot revert the EMT. This study was significant in identifying ROS as a crucial factor in both EMT and ferroptosis in the NMuMG cell line. These results can then, in the future contribute to further elucidate underlying mechanisms of key players involved in EMT and ferroptosis to overcome resistance of mesenchymal state cancer cells to therapies.

REFERENCES

1. UK CR. Cancer Statistics worldwide. 2021.
2. Hanahan D, Weinberg RA. Hallmarks of cancer: the next generation. Cell. 2011;144(5):646-74.
3. Fares J, Fares MY, Khachfe HH, Salhab HA, Fares Y. Molecular principles of metastasis: a hallmark of cancer revisited. Signal Transduct Target Ther. 2020;5(1):28.
4. Park M, Kim D, Ko S, Kim A, Mo K, Yoon H. Breast Cancer Metastasis: Mechanisms and Therapeutic Implications. Int J Mol Sci. 2022;23(12).
5. International WCRF. Worldwide cancer data 2023 [
6. Ye X, Weinberg RA. Epithelial-Mesenchymal Plasticity: A Central Regulator of Cancer Progression. Trends Cell Biol. 2015;25(11):675-86.
7. Huang Y, Hong W, Wei X. The molecular mechanisms and therapeutic strategies of EMT in tumor progression and metastasis. J Hematol Oncol. 2022;15(1):129.
8. Nieto MA. The ins and outs of the epithelial to mesenchymal transition in health and disease. Annu Rev Cell Dev Biol. 2011;27:347-76.
9. Lin YT, Wu KJ. Epigenetic regulation of epithelial-mesenchymal transition: focusing on hypoxia and TGF-β signaling. J Biomed Sci. 2020;27(1):39.
10. Kalluri R, Weinberg RA. The basics of epithelial-mesenchymal transition. J Clin Invest. 2009;119(6):1420-8.
11. Lamouille S, Xu J, Derynck R. Molecular mechanisms of epithelial-mesenchymal transition. Nat Rev Mol Cell Biol. 2014;15(3):178-96.
12. Katsuno Y, Lamouille S, Derynck R. TGF-β signaling and epithelial-mesenchymal transition in cancer progression. Curr Opin Oncol. 2013;25(1):76-84.
13. Barrallo-Gimeno A, Nieto MA. The Snail genes as inducers of cell movement and survival: implications in development and cancer. Development. 2005;132(14):3151-61.
14. Batlle E, Sancho E, Francí C, Domínguez D, Monfar M, Baulida J, et al. The transcription factor snail is a repressor of E-cadherin gene expression in epithelial tumour cells. Nat Cell Biol. 2000;2(2):84-9.
15. Yang J, Mani SA, Donaher JL, Ramaswamy S, Itzykson RA, Come C, et al. Twist, a master regulator of morphogenesis, plays an essential role in tumor metastasis. Cell. 2004;117(7):927-39.
16. Wang Y, Shi J, Chai K, Ying X, Zhou BP. The Role of Snail in EMT and Tumorigenesis. Curr Cancer Drug Targets. 2013;13(9):963-72.
17. Kurrey NK, Jalgaonkar SP, Joglekar AV, Ghanate AD, Chaskar PD, Doiphode RY, et al. Snail and Slug Mediate Radioresistance and Chemoresistance by Antagonizing p53-Mediated Apoptosis and Acquiring a Stem-Like Phenotype in Ovarian Cancer Cells. Stem Cells. 2009;27(9):2059-68.
18. Hojo N, Huisken AL, Wang H, Chirshev E, Kim NS, Nguyen SM, et al. Snail knockdown reverses stemness and inhibits tumour growth in ovarian cancer. Scientific Reports. 2018;8(1):8704.
19. Kaufhold S, Bonavida B. Central role of Snail1 in the regulation of EMT and resistance in cancer: a target for therapeutic intervention. Journal of Experimental & Clinical Cancer Research. 2014;33(1):62.
20. Fuertes G, Del Valle-Pérez B, Pastor J, Andrades E, Peña R, García de Herreros A, et al. Noncanonical Wnt signaling promotes colon tumor growth, chemoresistance and tumor fibroblast activation. EMBO Rep. 2023;24(4):e54895.

21. Xu J, Lamouille S, Derynck R. TGF-beta-induced epithelial to mesenchymal transition. Cell Res. 2009;19(2):156-72.
22. Chang Z, Zhang Y, Liu J, Zheng Y, Li H, Kong Y, et al. Snail promotes the generation of vascular endothelium by breast cancer cells. Cell Death Dis. 2020;11(6):457.
23. Dixon SJ, Lemberg KM, Lamprecht MR, Skouta R, Zaitsev EM, Gleason CE, et al. Ferroptosis: an iron-dependent form of nonapoptotic cell death. Cell. 2012;149(5):1060-72.
24. Ren Y, Mao X, Xu H, Dang Q, Weng S, Zhang Y, et al. Ferroptosis and EMT: key targets for combating cancer progression and therapy resistance. Cell Mol Life Sci. 2023;80(9):263.
25. Viswanathan VS, Ryan MJ, Dhruv HD, Gill S, Eichhoff OM, Seashore-Ludlow B, et al. Dependency of a therapy-resistant state of cancer cells on a lipid peroxidase pathway. Nature. 2017;547(7664):453-7.
26. Chen X, Li J, Kang R, Klionsky DJ, Tang D. Ferroptosis: machinery and regulation. Autophagy. 2021;17(9):2054-81.
27. Manz DH, Blanchette NL, Paul BT, Torti FM, Torti SV. Iron and cancer: recent insights. Ann N Y Acad Sci. 2016;1368(1):149-61.
28. Wu D, Yotnda P. Production and detection of reactive oxygen species (ROS) in cancers. J Vis Exp. 2011(57).
29. Maiorino M, Conrad M, Ursini F. GPx4, Lipid Peroxidation, and Cell Death: Discoveries, Rediscoveries, and Open Issues. Antioxid Redox Signal. 2018;29(1):61-74.
30. Doll S, Freitas FP, Shah R, Aldrovandi M, da Silva MC, Ingold I, et al. FSP1 is a glutathione-independent ferroptosis suppressor. Nature. 2019;575(7784):693-8.
31. Xu T, Ding W, Ji X, Ao X, Liu Y, Yu W, et al. Molecular mechanisms of ferroptosis and its role in cancer therapy. J Cell Mol Med. 2019;23(8):4900-12.
32. Zhang C, Liu X, Jin S, Chen Y, Guo R. Ferroptosis in cancer therapy: a novel approach to reversing drug resistance. Mol Cancer. 2022;21(1):47.
33. Liu RM, Desai LP. Reciprocal regulation of TGF-β and reactive oxygen species: A perverse cycle for fibrosis. Redox Biol. 2015;6:565-77.
34. Batlle E, Sancho E, Francí C, Domínguez D, Monfar M, Baulida J, et al. The transcription factor Snail is a repressor of E-cadherin gene expression in epithelial tumour cells. Nature Cell Biology. 2000;2(2):84-9.
35. Siddique YH, Ara G, Afzal M. Estimation of lipid peroxidation induced by hydrogen peroxide in cultured human lymphocytes. Dose Response. 2012;10(1):1-10.
36. Yang WS, SriRamaratnam R, Welsch ME, Shimada K, Skouta R, Viswanathan VS, et al. Regulation of ferroptotic cancer cell death by GPX4. Cell. 2014;156(1-2):317-31.
37. Zhou BP, Deng J, Xia W, Xu J, Li YM, Gunduz M, et al. Dual regulation of Snail by GSK-3β-mediated phosphorylation in control of epithelial–mesenchymal transition. Nature Cell Biology. 2004;6(10):931-40.
38. Riley L. Mean fasting blood glucose (mmol/L) (age-standardized estimate) world health organization [
39. TeSlaa T, Ralser M, Fan J, Rabinowitz JD. The pentose phosphate pathway in health and disease. Nature Metabolism. 2023;5(8):1275-89.
40. Liu X, Olszewski K, Zhang Y, Lim EW, Shi J, Zhang X, et al. Cystine transporter regulation of pentose phosphate pathway dependency and disulfide stress exposes a targetable metabolic vulnerability in cancer. Nat Cell Biol. 2020;22(4):476-86.
41. Patra KC, Hay N. The pentose phosphate pathway and cancer. Trends Biochem Sci. 2014;39(8):347-54.

42. Zhang H, Chen N, Ding C, Zhang H, Liu D, Liu S. Ferroptosis and EMT resistance in cancer: a comprehensive review of the interplay. Front Oncol. 2024;14:1344290.
43. Han X, Duan X, Liu Z, Long Y, Liu C, Zhou J, et al. ZEB1 directly inhibits GPX4 transcription contributing to ROS accumulation in breast cancer cells. Breast Cancer Research and Treatment. 2021;188(2):329-42.
44. Skouta R, Dixon SJ, Wang J, Dunn DE, Orman M, Shimada K, et al. Ferrostatins inhibit oxidative lipid damage and cell death in diverse disease models. J Am Chem Soc. 2014;136(12):4551-6.
45. Dibra D, Xiong S, Moyer SM, El-Naggar AK, Qi Y, Su X, et al. Mutant p53 protects triple-negative breast adenocarcinomas from ferroptosis in vivo. Sci Adv. 2024;10(7):eadk1835.
46. Miettinen PJ, Ebner R, Lopez AR, Derynck R. TGF-beta induced transdifferentiation of mammary epithelial cells to mesenchymal cells: involvement of type I receptors. J Cell Biol. 1994;127(6 Pt 2):2021-36.
47. Porsch H, Bernert B, Mehić M, Theocharis AD, Heldin CH, Heldin P. Efficient TGFβ-induced epithelial-mesenchymal transition depends on hyaluronan synthase HAS2. Oncogene. 2013;32(37):4355-65.
48. Boudreau HE, Casterline BW, Rada B, Korzeniowska A, Leto TL. Nox4 involvement in TGF-beta and SMAD3-driven induction of the epithelial-to-mesenchymal transition and migration of breast epithelial cells. Free Radic Biol Med. 2012;53(7):1489-99.
49. Liu RM, Gaston Pravia KA. Oxidative stress and glutathione in TGF-beta-mediated fibrogenesis. Free Radic Biol Med. 2010;48(1):1-15.
50. Bavarsad Shahripour R, Harrigan MR, Alexandrov AV. N-acetylcysteine (NAC) in neurological disorders: mechanisms of action and therapeutic opportunities. Brain Behav. 2014;4(2):108-22.
51. Garcia MA, Nelson WJ, Chavez N. Cell-Cell Junctions Organize Structural and Signaling Networks. Cold Spring Harb Perspect Biol. 2018;10(4).
52. Chen YH, Hsu JY, Chu CT, Chang YW, Fan JR, Yang MH, et al. Loss of cell-cell adhesion triggers cell migration through Rac1-dependent ROS generation. Life Sci Alliance. 2023;6(2).
53. Hall A. Rho GTPases and the control of cell behaviour. Biochem Soc Trans. 2005;33(Pt 5):891-5.
54. Yu H, Lee H, Herrmann A, Buettner R, Jove R. Revisiting STAT3 signalling in cancer: new and unexpected biological functions. Nat Rev Cancer. 2014;14(11):736-46.
55. Song S, Qiu D, Luo F, Wei J, Wu M, Wu H, et al. Knockdown of NLRP3 alleviates high glucose or TGFB1-induced EMT in human renal tubular cells. J Mol Endocrinol. 2018;61(3):101-13.
56. Sturrock A, Cahill B, Norman K, Huecksteadt TP, Hill K, Sanders K, et al. Transforming growth factor-beta1 induces Nox4 NAD(P)H oxidase and reactive oxygen species-dependent proliferation in human pulmonary artery smooth muscle cells. Am J Physiol Lung Cell Mol Physiol. 2006;290(4):L661-l73.
57. Shi L, Liu BY, Wang X, Zhu MJ, Chen L, Zhou MY, et al. RUNX3-dependent oxidative epithelial-to-mesenchymal transition in methamphetamine-induced chronic lung injury. Cell Stress Chaperones. 2020;25(5):793-802.
58. Chytła A, Gajdzik-Nowak W, Olszewska P, Biernatowska A, Sikorski AF, Czogalla A. Not Just Another Scaffolding Protein Family: The Multifaceted MPPs. Molecules. 2020;25(21).
59. Takada Y, Ye X, Simon S. The integrins. Genome Biol. 2007;8(5):215.

60. Lou Y, Jiang Y, Liang Z, Liu B, Li T, Zhang D. Role of RhoC in cancer cell migration. Cancer Cell Int. 2021;21(1):527.

ACKNOWLEDGEMENTS

I would like to thank my principal investigator Dr. Antonio Garcia de Herreros for being able to contribute to this research group and to gain more experience in research. I would like to give a special thanks to my daily supervisor Javier Pastor for the daily guidance, mentoring, support and being very patient with me during this whole experience teaching me many new techniques, etc. I would as well acknowledge all the members of the team for all the support and help in the lab during these months. Appreciation is extended to Dr. Leen Slaets, for the guidance during this period.

Autor contributions
J.P. and A.G.H. conceived and designed the research. A.T. did the experiments. A.T. and J.P. analyzed the data and writing the paper was done by A.T., J.P., and A.G.

SUPPLEMENTARY

Table 1 – Primers used for cDNA quantification

Gene	Forward (5'-3')	Reverse (5'-3')
Mouse		
Cdh1	TTCAACCCAAGCACGTATCA	ACGGTGTACACAGCTTTCCA
Fn1	AGCAAGCCTGAGCCTGAAGAG	GCGATTTGCAATGGTACAGCT
Gpx4	AGGAGCCCCAGGTGATAGAG	TATTCCCACAAGGCAGCCAG
Pum1	CGGTCGTCCTGAGGATAAAA	CGTACGTGAGGCGTGAGTAA
Snai1	GCGCCCGTCGTCCTTCTCGTC	CTTCCGCGACTGGGGGTCCT
Chac1	CTGTGGATTTTCGGGTACGG	CCCCTATGGAAGGTGTCTCC
Fth1	CCATCAACCGCCAGATCAAC	GCCACATCATCTCGGTCAAA
Vim	GGCTGCGAGAGAAATTGC	TCTCTTCATCGTGCAGTTTCTTC
Pten	GACAGCCATCATCAAAGAGATCG	GCAGTTAAATTTGGCGGTGT
Zeb1	TCAGCTGCTCCCTGTGCAGT	AAGGCCTTCCCGCATTCAGT

Table 2 – Primary antibodies western blot

Protein	Host	Dilution	Reference	Provider
β-actin	Rabit	1:10000	Ab8227	Abcam
E-cadherin	Mouse	1:1000	610182	BD Bioscience
Fibronectin1	Rabit	1:1000	Ab2413	Abcam
GPX4	Rabit	1:1000	Ab125066	Abcam
Snail	Rabit	1:1000	C1503	Cell signaling

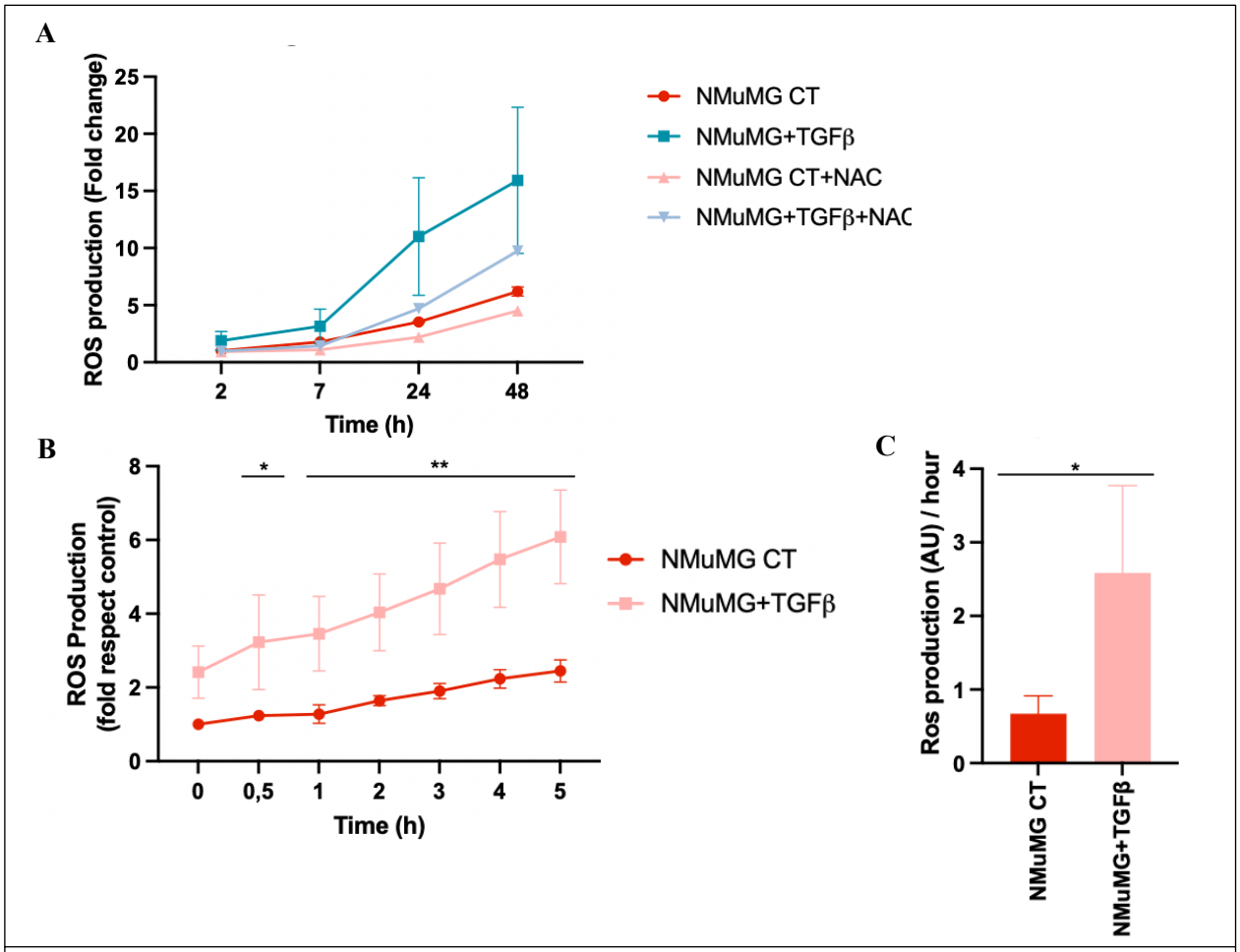

Fig. S1– Mesenchymal cells exhibit higher ROS levels compared to epithelial cells in HG. (A) ROS levels during EMT starting from 2 h until 48 h after EMT ± NAC (n=2). (B) ROS production levels 24 h after EMT was induced (n=4). (C) ROS production per hour HG (n=4). Data are means ± SEM. Significant differences were evaluated by analysis of variances (ANOVA). *P<0.05, **P<0.01.

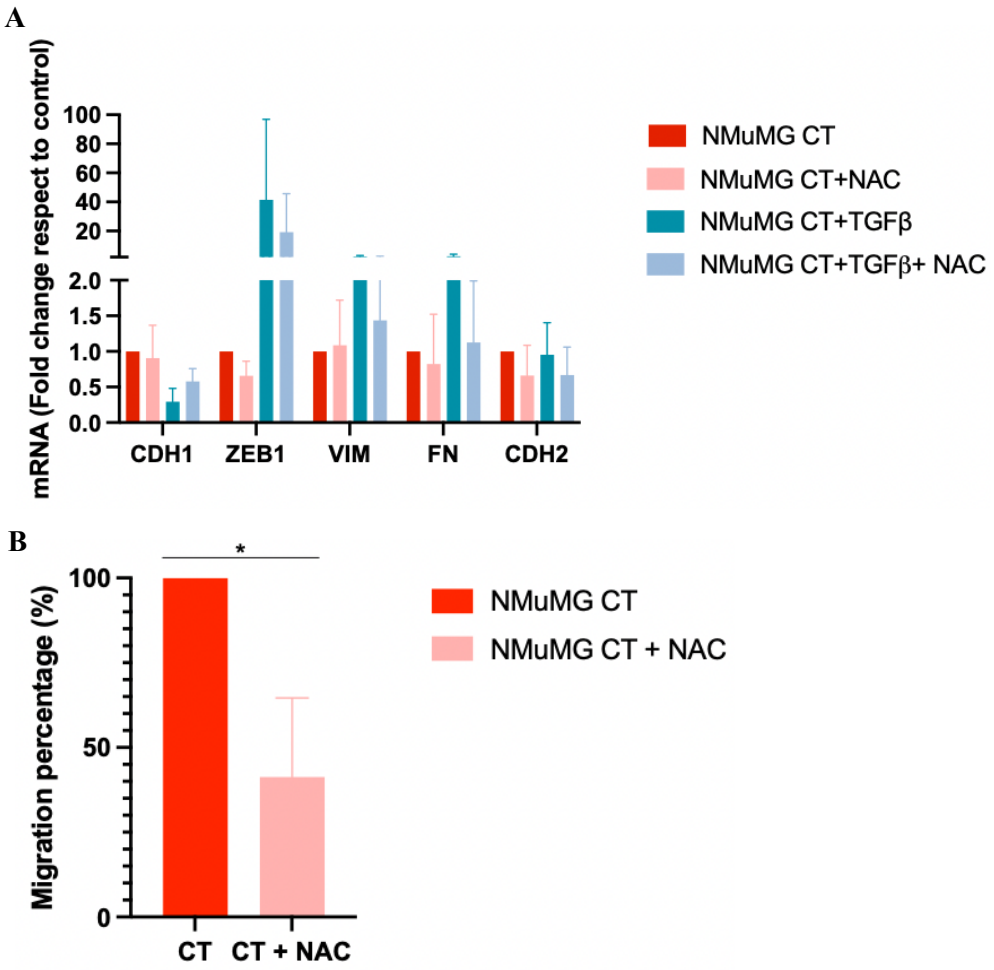

Fig. S2– Mesenchymal cells exhibit higher ROS levels compared to epithelial cells in HG. (A) qPCR plot of NMuMGs revealing the expression of mesenchymal markers (*Zeb1, Vim, Fn1* and *Cdh1*) and epithelial marker (*Cdh2*) in HG (n=2). (B) Transwell migration assay of NMuMG CT cells ± NAC (n=3). Data are means ± SEM. Significant differences were evaluated by analysis of variances (ANOVA). *P<0.05.